A new miniaturized multi-band transparent antenna for V2X communication

Omar Ourahou[1*], *Hassan Belahrach* [2], and Abdelilah Ghammaz[1]

[1]Department of Physics, Laboratory of Electrical systems, Energy efficiency and Telecommunications (LSEEET), Cadi Ayyad University, Marrakech, Morocco
[2]Laboratory of Electrical Engineering Royal School of Aeronautics Marrakesh, Morocco

Abstract. Intelligent transportation services are being developed to enhance road safety, increase traffic efficiency, achieve higher speeds, and alleviate traffic congestion. This article presents the design and simulation results of a novel, compact, transparent patch antenna. The suggested design is designed to cover vehicular communication standards such as DSRC/IEEE 802.11p at 5.9 GHz and cellular V2X (C-V2X) bands. Additionally, it supports other frequency bands, including the C-Band (5.925–6.425 GHz, 7.25-7.75 GHz) and X-Band (7.250-7.750 GHz, 7.90–8.40 GHz, 8.0–8.5 GHz). The antenna operates within the frequency ranges of 5.11–6.44 GHz and 7.25–9.06 GHz, achieving a gain of 2–5 dB and a radiation efficiency of approximately 90% at 5.9 GHz. The antenna is enhanced by adding slots to the patch and utilizing a modified ground plane.

1 Introduction

Extensive research has been conducted by industry and various organizations to enhance intelligent transportation systems (ITS) which can be improved by V2X communications[1]. The V2X which include vehicle-to-network (V2N), vehicle-to-pedestrian (V2P), vehicle-to-vehicle (V2V) and vehicle-to-infrastructure (V2I) communications can enhance road safety, increase traffic efficiency, achieve higher speeds, and alleviate traffic congestion[2]. DSRC based on IEEE 802.11p cellular V2X (C-V2X) are the main technology used in the world[3].

Despite their limited bandwidth, patch provide several benefits for wireless communication, such as their slim profile, seamless integration into peripheral devices, and cost-effectiveness [4]. Moreover, transparent antennas are highly appealing due to their broad range of applications, spanning defense, the Internet of Things (IoT), smart cities, security, healthcare, sports, vehicular communications, and various other domains [5].

In recent decades, antenna designers have primarily focused on reducing antenna size. Typically, the length of a standard antenna operating at a given frequency is approximately half the wavelength of that frequency [6].

The literature presents several methods for miniaturizing patch antennas, including material loading, shorting and folding, and introducing slots. The first approach achieves size reduction by adding slots or modifying the patch shape [7]. The second method, involving shorting and folding, focuses on deforming the ground plane, often using defected ground structures (DGSs) to minimize the antenna's size [8], [9]. The third and simplest technique is material loading, which uses a substrate with high relative permittivity (εr). However, this method leads to reduced bandwidth when a high εr substrate is used [10].

This paper presents a novel compact transparent antenna designed specifically for vehicular communications. The antenna design employs optimization techniques utilizing slots and defected ground plane structures (DGSs). It is engineered to support vehicular communication standards such as DSRC/IEEE 802.11p at 5.9 GHz and cellular V2X (C-V2X) bands, alongside broader compatibility with communication bands including C-Band and X-Band.

2 Antenna design and optimization

The proposed antenna is constructed on a plexiglass substrate with a thickness of 1.48 mm and a dielectric permittivity (εr) of 2.3. The patch and ground plane are fabricated from AgHT-8 conductor, which has a thickness of 0.177 mm and an electrical conductivity of 125,000 S/m.

The final geometry of the suggested design is presented in fig.1, and the final value of the dimension is given in Table.1.

Table 1. Optimal value of dimension of the proposed antenna

Dimension	Value(mm)	Dimension	Value(mm)
L1	20	W2	1.85
W1	20	W4	12
Lf	10	W3	1.5
Wf	2.9	L2	3.75
L3	8.5	h	1.48

* Corresponding author: Omar Ourahou (o.ourahou.ced@uca.ac.ma)

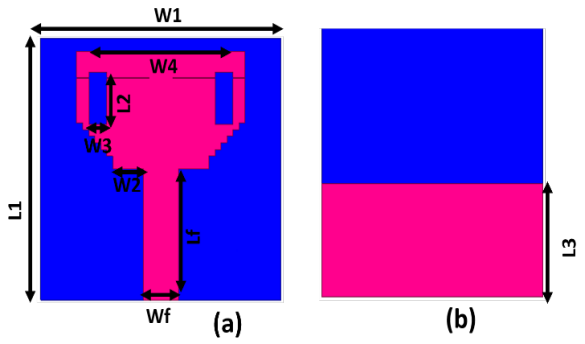

Fig. 1. Proposed antenna design (a) top view and (b) back view.

The design of the proposed antenna is demonstrated through a series of structural modifications to the patch, with each version shown in Fig. 2.

In the first stage, the antenna features a rectangular radiating element and a full ground plane, as shown in Fig. 2(e). At this stage, the antenna fails to operate at any frequency. In the second step, the ground plane is defected; however, the antenna still does not operate at the desired frequency. In the third iteration, several slots are introduced in the radiating patch. The antenna is observed to operate at a frequency of 6.5 GHz. By incorporating additional slots in the radiating patch, the electrical length is extended, shifting the resonant frequency to lower values. As a result, the antenna functions at 5.9 GHz, a frequency designated for V2X communications.

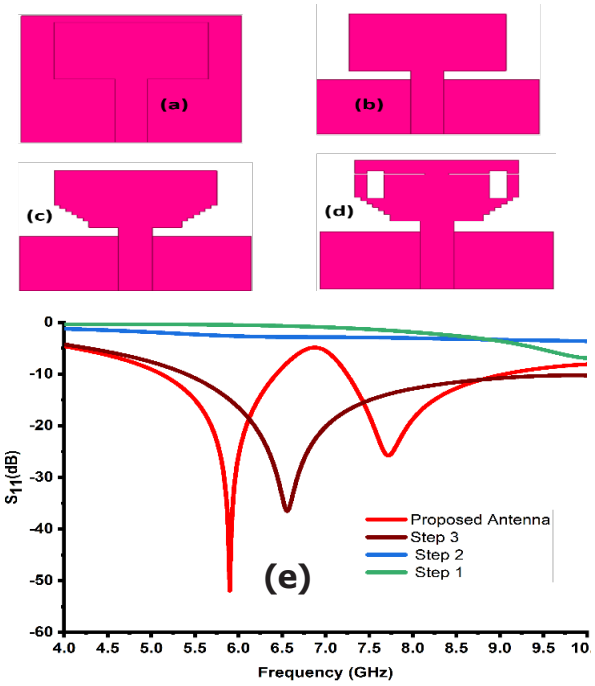

Fig. 2. Design evolution (a) Step1, (b) Step2, (c) Step3, (d) Proposed Antenna, and (e) correspond return loss coefficient.

The parametric analysis offers a detailed insight into how changes in numerical values of various variables affect the antenna's performance. This study is essential in determining the key parameters that optimize the antenna to meet its intended functionality.

The key parameters that optimize the antenna to meet its intended functionality.

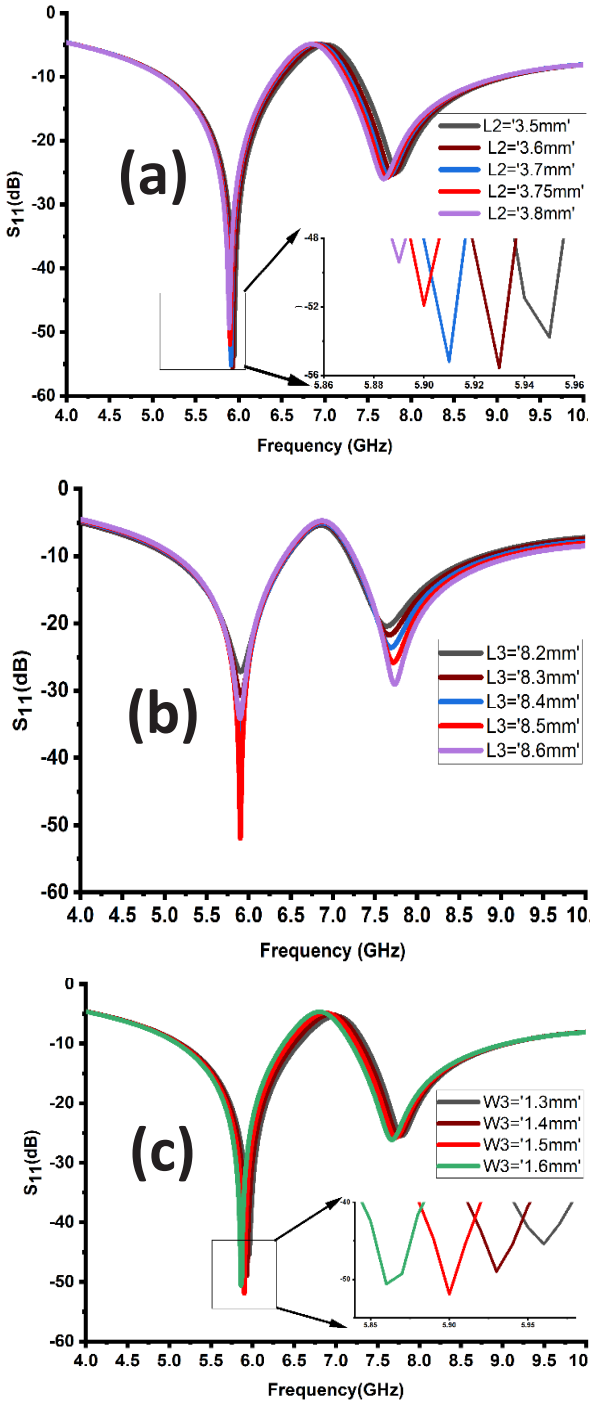

Fig. 3. Effect of parameters on return loss coefficient: (a) effect of L2, (b) effect of L3, and (c) effect of W3.

Fig. 3(a) demonstrates the influence of the slot length 'L2' on the resonant frequency. As 'L2' increases, the resonant frequency shifts to lower values. Conversely, reducing 'L2' causes the resonant frequency to shift to higher values. The optimal length of 'L1' for achieving a resonant frequency of 5.9 GHz is determined to be 3.75 mm, indicating a precise tuning capability through 'L1' adjustments.

Fig.3(b) depicts the impact of ground length 'L3' on the S11 value, showing a decrease in S11 as 'L3' increases. The optimal S11 is attained when 'L3' reaches

8.5 mm, indicating that the ground length 'L3' is critical for impedance matching and reducing return loss.

Fig.3(c) shows the effect of slot width 'W3' on the return loss coefficient. As 'W3' increases, the resonant frequency shifts to a lower value. The optimal value for 5.9 GHz is achieved when 'W2' is 1.5 mm, highlighting the importance of 'W2' in tuning the resonant behavior and obtaining the desired performance.

3 Results and discussion

This section presents the findings for the return loss coefficient, VSWR, gain, efficiency, and radiation pattern. The simulations were performed using HFSS software.

Fig.4(a) shows the return loss coefficient of the proposed antenna, which operates across two distinct frequency bands. The first band extends from 5.11 GHz to 6.44 GHz, offering a bandwidth of 1.33 GHz, while the second band ranges from 7.25 GHz to 9.06 GHz, providing a bandwidth of 1.81 GHz. The antenna exhibits a resonant frequency at 5.9 GHz with an |S11| value of -52 dB, indicating excellent impedance matching and minimal signal reflection. A second resonance occurs at 7.72 GHz with an S11 value of -25 dB.

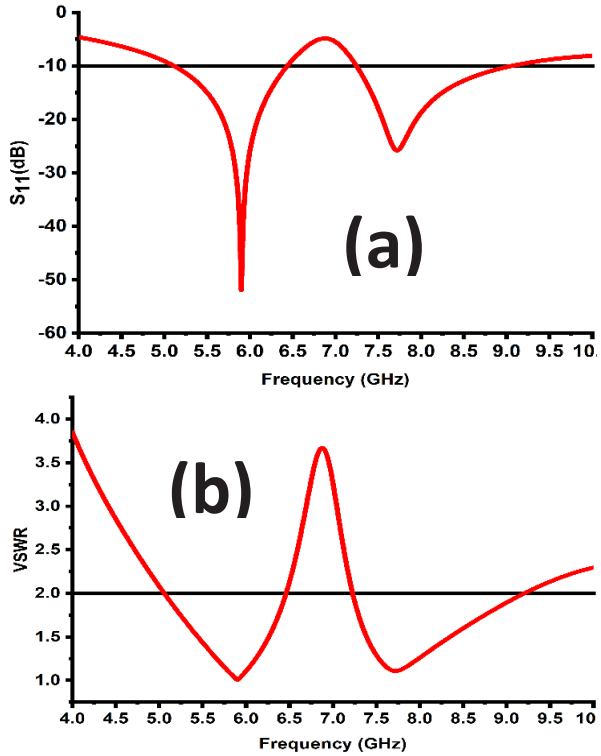

Fig. 4. Return loss coefficient of the proposed antenna in (a) VSWR in (b).

Fig.4(b) illustrates the Voltage Standing Wave Ratio (VSWR) of the antenna system. The data indicates that the proposed antenna achieves excellent performance, with VSWR values remaining below 2 across the operating bandwidths. This demonstrates effective impedance matching and efficient power transfer.

Fig.5 displays the simulated radiation patterns of the proposed antenna in the H-Plane (Phi = 90.00°) and E-Plane (Phi = 0.0°) at frequencies of 5.9 GHz and 7.7 GHz. For DSRC applications, antennas typically require an omnidirectional radiation pattern in the azimuthal plane. The simulated patterns show that the proposed antenna provides omnidirectional radiation at both resonant frequencies, making it well-suited for vehicular communications.

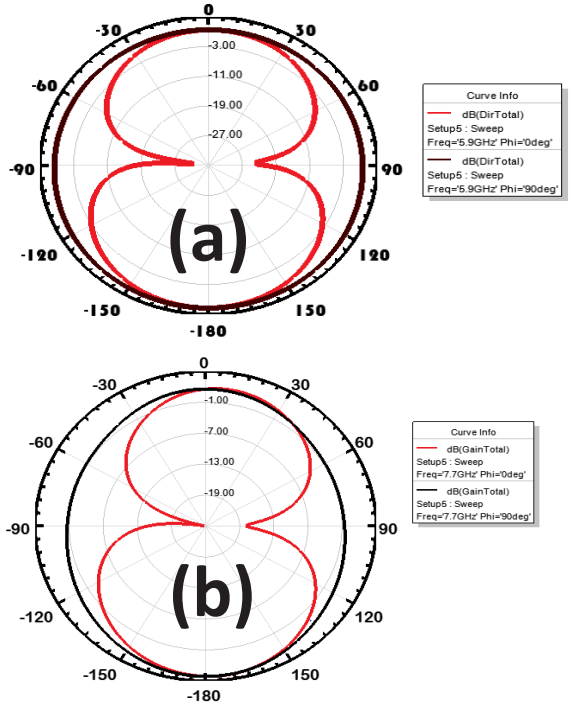

Fig. 5. 2D radiation pattern of the proposed antenna (a) at 5.9 GHz, and (b) at 7.7 GHz.

Fig.6 displays the simulated gain and radiation efficiency. The simulated gain measures approximately 3 dB at 5.9 GHz and around 4.5 dB at higher frequencies. Moreover, the simulated efficiency remains consistently high, at approximately 90% across the operating band.

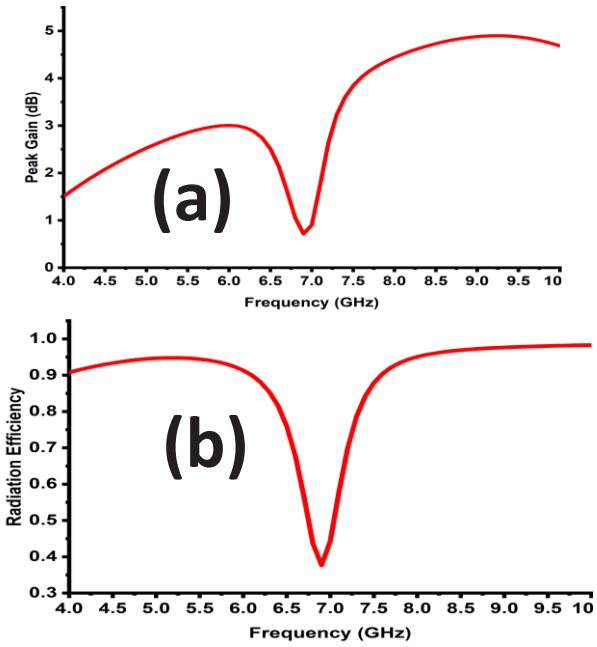

Fig. 6. Peak gain of the proposed antenna in (a) and radiation efficiency in (b).

Table 2. Comparison of antenna performance with existing work

Reference	Dimension (mm)	Operating band (GHz)	Gain (dB)	Efficiency
[11]	-	5.85–5.9250	5.0	-
[3]	40×40×1.60	5.9	-	-
[12]	60×86×0.6	5.85–5.95	8.3	99.6
[13]	50×50×1.60	2.350–3.61 5.15–6.25	2.8–3.50 3.7–4.30	-
[14]	80 × 80	5.84-6.01	6.3	-
[15]	31× 28 ×1.6	3.22-6.5	3.20	-
Proposed antenna	20×20×1.48	5.11-6.44 7.25-9	3 4	90% 95%

4 Conclusion

A new bi-band compact transparent antenna is presented, studied, and analyzed in this work. The antenna is engineered to operate within vehicular communication bands, encompassing cellular V2X (C-V2X), DSRC/IEEE 802, and various other wireless applications. Slots and a defected ground plane are utilized to miniaturize the proposed antenna, making it more attractive in both appearance and functionality. The proposed antenna operates in the 5.11-6.44 GHz band and the 7.25-9.06 GHz band, with an average gain of approximately 3 dB and 4.5 dB, respectively. Due to its aesthetic design, the antenna is suitable for integration into various locations within a vehicle, such as the windshield or window.

Reference

1. S. Chen *et al.*, “Vehicle-to-Everything (v2x) Services Supported by LTE-Based Systems and 5G,” *IEEE Communications Standards Magazine*, vol. 1, no. 2, pp. 70–76, 2017, doi: 10.1109/MCOMSTD.2017.1700015.
2. S. Gyawali, S. Xu, Y. Qian, and R. Q. Hu, “Challenges and Solutions for Cellular Based V2X Communications,” *IEEE Communications Surveys and Tutorials*, vol. 23, no. 1, pp. 222–255, Jan. 2021, doi: 10.1109/COMST.2020.3029723.
3. F. Ez-Zaki *et al.*, “Double Negative (DNG) Metamaterial-Based Koch Fractal MIMO Antenna Design for Sub-6-GHz V2X Communication,” *IEEE Access*, vol. 11, pp. 77620–77635, 2023, doi: 10.1109/ACCESS.2023.3296599.
4. B. D. Pell, E. Sulic, W. S. T. Rowe, K. Ghorbani, and S. John, “26 Advancements in Automotive Antennas.” [Online]. Available: www.intechopen.com
5. A. S. M. Sayem, A. Lalbakhsh, K. P. Esselle, J. L. Buckley, B. O’Flynn, and R. B. V. B. Simorangkir, “Flexible Transparent Antennas: Advancements, Challenges, and Prospects,” *IEEE Open Journal of Antennas and Propagation*, vol. 3, no. September, pp. 1109–1133, 2022, doi: 10.1109/OJAP.2022.3206909.
6. M. Boudjerda *et al.*, “Design and Optimization of Miniaturized Microstrip Patch Antennas Using a Genetic Algorithm,” *Electronics (Switzerland)*, vol. 11, no. 14, Jul. 2022, doi: 10.3390/electronics11142123.
7. C. Kalialakis, “Planar Antennas for Wireless Communications [Book Review],” *IEEE Antennas Propag Mag*, vol. 46, no. 1, 2004, doi: 10.1109/map.2004.1296156.
8. M. S. Sharawi, M. U. Khan, A. B. Numan, and D. N. Aloi, “A CSRR loaded MIMO antenna system for ISM band operation,” *IEEE Trans Antennas Propag*, vol. 61, no. 8, 2013, doi: 10.1109/TAP.2013.2263214.
9. J. X. Liu, W. Y. Yin, and S. L. He, “A new defected ground structure and its application for miniaturized switchable antenna,” *Progress in Electromagnetics Research*, vol. 107, 2010, doi: 10.2528/PIER10050904.
10. T. AlSharabati, “Microstrip patch antenna miniaturization using magneto-dielectric substrates for electromagnetic energy harvesting,” *Journal of Communications Software and Systems*, vol. 17, no. 2, 2021, doi: 10.24138/jcomss-2020-0005.
11. M. Westrick, M. Almalkawi, V. Devabhaktuni, and C. Bunting, “A low-profile, low-cost antenna system with improved gain for DSRC vehicle-to-vehicle communications,” *International Journal of RF and Microwave Computer-Aided Engineering*, vol. 23, no. 1, pp. 111–117, Jan. 2013, doi: 10.1002/mmce.20657.
12. K. Aliqab, A. Armghan, M. Alsharari, and M. H. Aly, “Highly decoupled and high gain conformal two-port MIMO antenna for V2X communications,” *Alexandria*

Engineering Journal, vol. 74, pp. 599–610, Jul. 2023, doi: 10.1016/j.aej.2023.05.058.

13. J. Ali *et al.*, "Cantor fractal-based printed slot antenna for dual-band wireless applications," *Int J Microw Wirel Technol*, vol. 8, no. 2, pp. 263–270, Mar. 2016, doi: 10.1017/S1759078714001469.
14. A. Pal and V. S. Tripathi, "Quad-element MIMO antenna with diverse radiation pattern characteristics and enhanced gain for 5.9 GHz V2X communications," *AEU - International Journal of Electronics and Communications*, vol. 176, Mar. 2024, doi: 10.1016/j.aeue.2024.155119.
15. F. Ez-Zaki, H. Belahrach, and A. Ghammaz, "Broadband microstrip antennas with Cantor set fractal slots for vehicular communications," *Int J Microw Wirel Technol*, vol. 13, no. 3, pp. 295–308, Apr. 2021, doi: 10.1017/S1759078720000719.